Since January 2020 Elsevier has created a COVID-19 resource centre with free information in English and Mandarin on the novel coronavirus COVID-19. The COVID-19 resource centre is hosted on Elsevier Connect, the company's public news and information website.

Journal of Infection and Public Health 13 (2020) 1142–1147

Contents lists available at ScienceDirect

Journal of Infection and Public Health

journal homepage: http://www.elsevier.com/locate/jiph

Original Article

A three-dimensional A549 cell culture model to study respiratory syncytial virus infections

Fatima Saleh[a,1], Aya Harb[b,1], Nadia Soudani[b,c,d], Hassan Zaraket[b,c,*]

[a] Department of Medical Laboratory Sciences, Faculty of Health Sciences, Beirut Arab University, Lebanon
[b] Faculty of Medicine, Department of Experimental Pathology, Immunology & Microbiology, American University of Beirut, Beirut, Lebanon
[c] Faculty of Medicine, Center for Infectious Diseases Research, American University of Beirut, Beirut, Lebanon
[d] Doctoral School of Sciences and Technology, Research Platform for Environmental Science (PRASE), Faculty of Sciences, Lebanese University, Lebanon

ARTICLE INFO

Article history:
Received 29 November 2019
Received in revised form 10 March 2020
Accepted 16 March 2020

Keywords:
Respiratory syncytial virus (RSV)
3D culture
A549
Infection
Mucin

ABSTRACT

Background: Respiratory syncytial virus (RSV) is a primary cause of morbidity and mortality worldwide, affecting infants, young children, and immune-compromised patients; however, currently no vaccine is available for prevention of RSV infections. The overwhelming majority of our knowledge of how RSV causes infection is based upon studies that have been carried out using traditional 2D methods, with cells cultured on flat plastic dishes. Although these simplified culture systems are essential to gain an insight into the fundamentals of host-pathogen interactions, cells in 2D are not exposed to the same conditions as cells in 3D tissues in the body and are therefore a poor representation of the*in vivo* microenvironment. In this study, we aim to develop the first 3D culture model for RSV infection using A549 cells to test its utility for RSV pathogenesis.
Methods: To generate spheroids, A549 cells were cultured using ultra-low attachment plates to generate 25×10^3 cell spheroids. The viability of the spheroids was assessed by trypan blue exclusion assay and flow cytometry showing prominent live cells throughout the spheroids confirming high viability over seven days of incubation.
Results: Immunostaining of A549 spheroids inoculated with RSV, showed time-dependent dissemination of the viral antigen RSV-F within the spheroid, resulting in syncytia formation and a 3-fold increase in mucin secretion compared to the uninfected cells. Additionally, RSV successfully replicated in the spheroids producing infectious virus as early as day one post-inoculation and was sustained for up to 7 days post-inoculation.
Conclusions: Results show that A549 spheroids are susceptible and permissive for RSV since they exhibit the characteristics of RSV infection including syncytia formation and mucin overexpression, suggesting that A549 spheroids can be used a promising model for studying RSV *in vitro*.

Introduction

Respiratory syncytial virus (RSV) is one of the major causes of pediatric respiratory tract infections [1]. RSV is estimated to cause approximately 30.5 million annual cases among infants less than one, of which 3.3 million require hospitalization [1]. We have recently shown that RSV accounts for 16% of influenza-like illnesses in Lebanon, where children under the age of 2 years were at the highest risk for infection [2]. Recurrent infections later in life are inevitable and are usually asymptomatic or accompanied by mild symptoms [3].

RSV is an enveloped *Pneumovirus* belonging to the *Paramyxoviridae* family with a linear, non-segmented, single-stranded, (−) sense RNA genome coding for 11 viral proteins [4]. The two envelop proteins, glycoproteins G and fusion protein F constitute the viral antigens that trigger the humoral and cellular immune response of the host [5]. The G protein mediates attachment of RSV to its host cell, while the F protein triggers the fusion of the viral envelop with the cell plasma membrane during viral penetration. Moreover, the F protein mediates the fusion between neighboring cells resulting

* Corresponding author at: Faculty of Medicine, Department of Experimental Pathology, Immunology & Microbiology, American University of Beirut, Riad El Solh, Beirut 1107 2020, Lebanon.
E-mail address: hz34@aub.edu.lb (H. Zaraket).
[1] These authors contributed equally to the work.

https://doi.org/10.1016/j.jiph.2020.03.011

in syncytia formation, which is the most common method of virus propagation [5].

RSV infection starts as a mild upper respiratory tract infection [6,7]. However, the infection can progress to lower respiratory tract infection, characterized by severe symptoms and pathogenesis such as epithelial cell necrosis, sloughing of desquamated cells into the bronchiolar lumen, submucosal and adventitial tissue edema as well as accumulation of macrophages and neutrophils in the peribronchiolar and perivascular regions [8]. Besides, excessive mucus secretion and syncytia formation represent the main hallmarks of RSV infection [8,9]. Excessive mucus secretion upon RSV infection leads to the formation of mucus plugs, pulmonary obstruction, and shortness of breath [10].

Most of the data currently available on RSV are from studies in monolayer (2D) cultures. 2D cell culture models lack the complex biological processes that occur *in vivo*; therefore, the pathogenesis of RSV in these flat models may not be representative of what happens *in vivo* [11,12]. Studies have demonstrated that cells undergo different biologic responses when grown in 3D compared with 2D settings [13,14]. They can differ in their morphology, with an altered cytoskeletal organization and cell adhesion. Other changes include different proliferation rates, signaling processes and differentiation potential. Many of these differences are believed to result from the fact that cells grown as monolayers on flat plastic surfaces are not subjected to the cell–cell and cell–matrix interactions, soluble factors, matrix composition and stiffness, oxygen and nutrient gradients, protein concentration gradients and mechanical stresses, as they would in their source tissues [10].

Since the early 2000s, an increasing number of evidence emerged about 3D cell cultures remarkably recapitulating the host cell response to microbial infections *in vivo* [15–17]. 3D cultures have been successful in studying various viruses and were the first definitive model for human norovirus and hepatitis C virus; however, to date, there are no reports to investigate RSV growth and pathogenesis in 3D cultures [17–19]. In this study, a scaffold-free 3D culture system was adopted using ultra-low attachment (ULA) plates to generate a practical and economic A549 spheroids model and test its permissiveness to RSV.

Materials and methods

Cell culture

African green monkey kidney cells (Vero cells, ATCC CCL-81), human Alveolar epithelial type II cells (A549; ATCC CCL-185) and human laryngeal carcinoma cells (Hep2 cells, ATCC CCL-23, a kind gift from Dr. Ralph Tripp, University of Georgia) were cultured in Dulbecco modified Eagle medium-high glucose (DMEM, D5796-Sigma) supplemented with 10% fetal bovine serum (F9665-Sigma) and 1% of 100 U/ml penicillin/streptomycin (pen/strep, MS006W100N Biowest) and maintained in 5% CO_2 at 37 °C.

A549 spheroid formation

A549 cells cultured in monolayers were dissociated and suspended in complete medium containing 0.25% methylcellulose (M0512-Sigma) as a thickening agent [20]. Seeding densities of 10×10^3, 25×10^3 or 50×10^3 cells were prepared in 200 μl of the 0.25% methylcellulose nutritive medium and seeded in 96-well round-bottom ultra-low attachment (ULA) plates (7007 Corning). Each well forms a single spheroid whose size varies depending on the initial cell seeding density. The cells were then incubated for seven days with media change every other day for the duration of the experiment.

Spheroid viability

A549 Spheroids' growth and viability were assessed on days 3, 5, and 7 post-seeding. The culture media was aspirated, and spheroids were washed with 1X PBS (D1408-500 ml Sigma). The spheroids were dissociated into single-cell suspensions by treatment with 0.25% trypsin/ EDTA (T4049-500 ml Sigma) for 15 min, followed by gentle pipetting. Then complete media was added, and the single-cell suspensions of the corresponding spheroids were centrifuged at 1100 RPM for 5 min. The cell pellets were resuspended in 300 μl of 1:1 mixture of complete media and trypan blue (T8154-100 ml Sigma). Viable cell count was determined using a hemocytometer. Alternatively, the cell pellets were resuspended in a 0.02 μM calcein-AM solution (C3099 Life Technologies) and incubated at room temperature for 20 min in the dark. Following incubation, the cells were pelleted, resuspended in 800 μl of PBS and passed through the Guava EasyCyte8 Flow Cytometer. A total of 5000 live events were excited at 488 nm per sample and measured for green fluorescence at 530 nm. Gating analysis was performed using FlowJo (FlowJo LLC) cytometry analysis software and a representative density-plot graph was shown.

Virus propagation and titration

Vero cells were used for virus propagation. These cells were inoculated with human RSV subgroup A (RSVA 2001/2–20, IRR) at 0.5 multiplicity of infection (MOI). The virus was then harvested upon extensive syncytia formation (5–8 days) by a single freeze-thaw lysis cycle followed by centrifugation and collection of the supernatant. The virus stock was quantified by using plaque assay. In brief, Hep2 cells seeded on a 6-well plate were inoculated with 200 μl of 10-fold serial dilutions of the virus stock for 2 h with gentle shaking every 15 min. Afterward, the cells were covered with 2 ml of newly prepared 0.15% agarose nutritive overlay and incubated for 7 days. Plaques were visualized by staining the cells with a crystal violet solution containing 5% formaldehyde.

Infectivity and growth kinetics of RSV in 3D spheroids

Three-day-old A549 spheroids were inoculated using RSV at a MOI = 1 (in a volume of 20 μl) and incubated for 2 h to allow virus adsorption. The inoculum was then removed and the spheroids were washed with DMEM and incubated for 7 days in 200 μl of DMEM containing 5% FBS and 1% pen/strep. Plaque assay was used to assess the spheroids' infectious virus yield at days 1, 3, 5 and 7 post-inoculation. At each time point, five spheroids were pooled with their supernatant, broken down into cell suspensions by vigorous pipetting and cells lysed by flash freezing to ensure the release of virions from the cells. The resulting cell lysate was then centrifuged and the plaque assay was performed on the supernatant as shown above to determine the viral yield in terms of plaque forming units (pfu) per milliliter (ml).

Immunofluorescent staining of spheroids

After 3 and 7 days post-inoculation, spheroids were fixed with 4% paraformaldehyde (416785000 ACROS) for 15 min and permeabilized with 0.2% Triton X-100 (T9284-100 ml Sigma) in PBS for 20 min. Spheroids were blocked with blocking solution [1% BSA (A3912-100 g Sigma) and 0.1% Triton X-100 in PBS] for 1 h followed by overnight incubation with a mixture of mouse anti-RSV fusion protein antibody (MAB8599-Merck Millipore) at 1:200 and rabbit anti-human MUC1 antibody (12123-T24

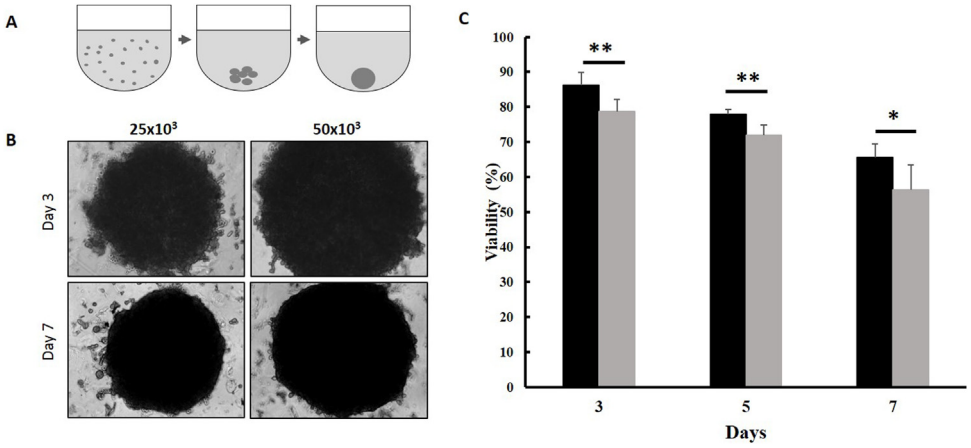

Fig. 1. Morphology and viability of A549 spheroids in U-bottom, 96-well ULA plates. (1A) Schematic diagram of spheroid assembly. (1B) Phase-contrast optical micrographs showing A549 spheroids morphology at an initial seeding density of 25 × 10^3 and 50 × 10^3 cells/well after 3 and 7 days of culture. (1C) Influence of culture time on the viability of A549 spheroids at a seeding density of 25 × 10^3 cells/well (black bars) and 50 × 10^3 cells/well (grey bars). At days 3, 5, and 7 post-seeding, spheroids were dissociated, stained with trypan blue, and counted under the microscope using a hemocytometer. 25 × 10^3 A549 spheroids reveal significantly higher viability than the 50 × 10^3 A549 spheroids at all time-points. Error bars represent ± SD (n = 6). *$p < 0.05$, ** $p < 0.01$.

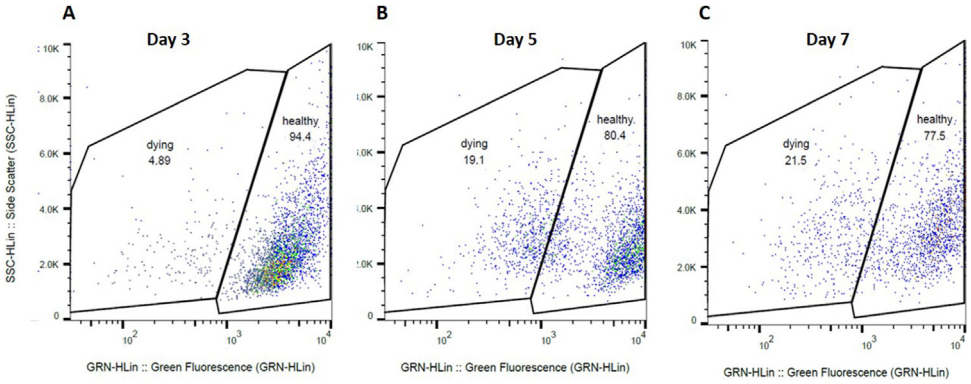

Fig. 2. Flow cytometry analysis of 25 × 10^3 A549 spheroids. Spheroids were cultured for 3, 5, and 7 days, then dissociated into single-cell suspensions, stained with 0.02 μM calcein-AM, and underwent flow cytometry at 488 nm excitation (n = 3). Density plots displaying calcein-AM florescent cells *versus* side scatter (SSC) illustrated 94.4% viability at day 3 (2A), 80.4 % viability at day 5 (2B) and 77.5 % viability at day 7 (2C). The analysis was performed by Flow Jo software.

Sino Biological) at 1:2500 in blocking buffer. The samples were then thoroughly washed with PBS/Tween (0.1%) (BP337-500-Fisher BioReagents) and incubated for 1 h with the corresponding fluorescent secondary antibodies (1:250) [Alexa fluor 488-goat anti-mouse IgG antibody (A11002-Life Technologies) and Alexa fluor 594-donkey anti-rabbit IgG antibody (A21207-Life Technologies)]. Finally, the immunostained spheroids were mounted with the Fluoroshield with DAPI histology mounting medium (F6057-Sigma), before being visualized by the LSM710 laser scanning confocal microscope (Zeiss). The fluorescence intensities of MUC1 and RSV-F captured on the images were quantified by employing ZEN blue edition (Zeiss) and presented as fold change values in infected spheroids as compared to their time matching controls.

Statistical analysis

All experiments were done at least two times in triplicates (unless otherwise indicated) and the data were presented as mean ± SD. The statistical significance of differences between groups was performed by Student's t-test using SPSS statistical software version 24 (SPSS, Inc., Chicago, IL, USA). A P-value <0.05 was considered to indicate a statistically significant difference.

Results

Generation of A549 spheroids using ultra-low attachment (ULA) plates

Three starting cell-seeding densities were used; namely, 10 × 10^3, 25 × 10^3, and 50 × 10^3 cells/well in 96 well, ultra-low attachment (ULA) plates (Fig. 1A), and the resulting spheroids were followed up until day 7 in culture. Well-formed spheroids were visible for the 25 × 10^3 and 50 × 10^3 cell seeding densities at day 3 post-seeding, becoming more compact on day 7 (Fig. 1B). However, the 10 × 10^3 cell seeding density failed to produce well-formed spheroids even after 7 days of incubation and therefore were abandoned.

The cell count and viability of spheroids were assessed using trypan blue exclusion assay (Fig. 1C). Three days post-seeding, the 25 × 10^3 spheroids grew to reach ~33 × 10^3 viable cells (86% viability). The 50 × 10^3 cell spheroids contained 37 × 10^3 viable cells (78% viability). Throughout the 7 days, the 25 × 10^3 cell spheroids maintained a constant viable cell count of ~33 × 10^3 cells, although their viability gradually yet significantly decreased, reaching 65% by day 7 (Fig. 1C). As for the 50 × 10^3 cell spheroids, a gradual and significant decline in viability was recorded throughout the 7 days. The viable cell count significantly dropped to 18 × 10^3 cells only

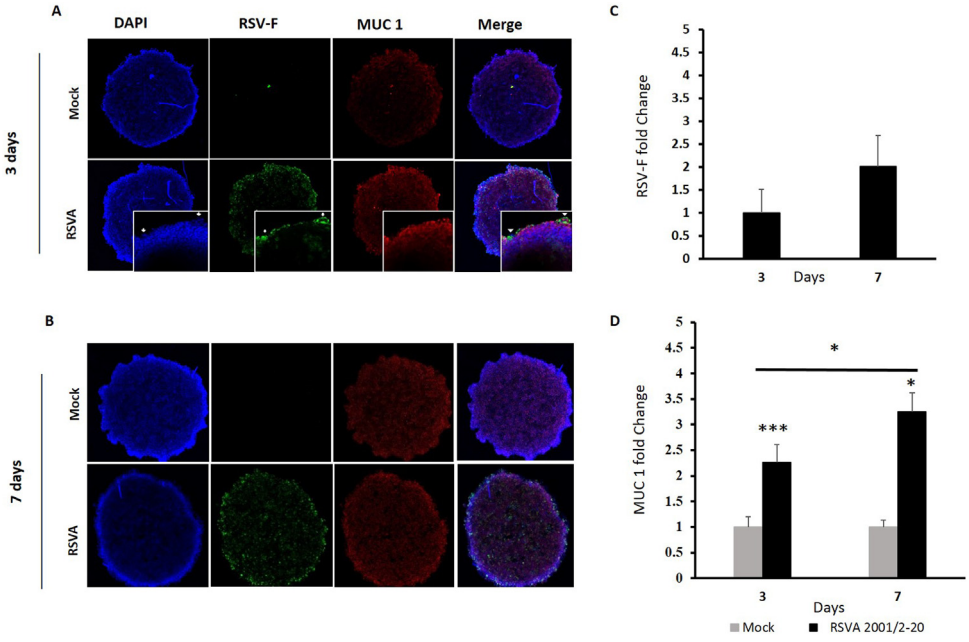

Fig. 3. RSVA infection and mucin production in A549 spheroids. A549 Spheroids were inoculated with 1 MOI of RSVA 2001/2-20 and incubated for 3 (3A) and 7 (3B) days. At the assigned time-points, spheroids were immunostained with anti-RSV F antibody (green), anti-MUC1 antibody (red), and counterstained with the nuclear stain DAPI (blue) and visualized by confocal microscopy at 10× magnification (n = 3). Syncytial formation in RSV infected spheroids at day 3 post-infection was also shown in insets at 40× magnification. (3C) Mucin accumulation and (3D) RSV-F dissemination were measured by the Zeiss LSM710 laser scanning confocal microscope. Mucin intensity fold change was evaluated between infected spheroids and their time matching controls (n = 3). RSV-F intensity fold change was evaluated between day 3 and day 7 infected spheroids (n = 3). Error bars represent ± SD (n = 3). $^{*}p < 0.05$, $^{**}p < 0.01$, $^{***}p < 0.001$.

by day 7 with 56% viability. Comparative viability analysis of the 25×10^3 and 50×10^3 cell spheroids showed significantly lower viability of the bigger spheroids than the smaller ones. Therefore, the 25×10^3A549 spheroids were adopted for the rest of the study.

The viability profile of 25×10^3 cell spheroids was further validated using flow cytometry. Similar to the data obtained by using trypan blue, we observed a steady time-dependent decline in the viability of the spheroids between days 3 to 7, where the healthy population dropped from 94.4% to 77.5%, respectively (Fig. 2).

RSV infection of A549 spheroids

We next sought to determine if the A549 spheroids are susceptible and permissive for RSV infection. As such, 3-day-old spheroids were inoculated with RSV (1 MOI) and immunostained at days 3 and 7 post-inoculation (Fig. 3). A prominent RSV-F protein staining was noted at day 3 post-inoculation (Fig. 3A) that disseminated towards the core of the spheroid by day 7 post-inoculation (Fig. 3B). Mild syncytia formation induced by RSV infection was also noted at the spheroid rim at 3 days post-inoculation (Fig. 3A insets). The intensity of RSV-F protein staining increased by 2-fold on day 7 compared to day 3 post-inoculation (Fig. 3C). These findings indicate that the virus has effectively infected the spheroids spreading towards its center throughout infection. Additionally, a 2.6-fold increase in MUC1 expression was noted in the spheroids on day 3 post-infection compared to mock (uninfected). MUC1 production further increased, reaching 3.25-fold at day 7 post-inoculation relative to mock (Fig. 3D). These results are indicative of a progressive infection established in the form of virus dissemination within the spheroids and gradual mucin accumulation, a hallmark of RSV infection.

After establishing and demonstrating successful infection of spheroids with RSV, plaque assay was performed to investigate growth kinetics of RSV in spheroids after 1, 3, 5, and 7 days of infection (Fig. 4). The data revealed productive viral replication in the spheroids, yielding 5.25 $\log_{10}$ PFU/ml unit at day 1 post-inoculation. The virus yield slightly dropped from 4.93 $\log_{10}$ at day 3 and reaching 4 $\log_{10}$ PFU/ml on days 5 and 7 post-inoculation, suggesting that spheroids are capable of sustaining infection for up to 7 days post-inoculation.

Discussion

Animal models have been routinely used to study RSV-induced respiratory diseases; even though useful, they do not fully mimic viral pathogenesis *in vivo* [21–26]. This can be attributable to the molecular, cellular, and physiological differences between animals and humans. 3D culture techniques have been used for many years in a wide variety of biomedical applications ranging from cancer and stem cell biology to tissue engineering and regenerative medicine [17,27–32]. 3D cultures promote direct cell-cell contact, interactions of cells with the extracellular matrix (ECM), and *in vivo*-like exchange of soluble factors, thus allowing cells to more closely resemble the *in vivo* parental tissue as opposed to their 2D monolayer counterparts [13–15]. Despite their success, the use of 3D technology in studying microbial infections is still in its infancy.

3D culture models have well demonstrated utility for studying bacterial and viral pathogens. Previous studies revealed that spheroids are more representative models for *Pseudomonas aeruginosa* and *Salmonella enterica* compared to monolayer cultures in terms of invasiveness, histopathology, and immunopathology [33,34]. Cells grown in spheroids were also shown to be the first definitive model for human norovirus [18] and hepatitis C virus studies [19], which lacked a suitable cell culture and murine study models. These viruses were capable of replicating and triggering a cytopathic effect in the 3D spheroid. Moreover, influenza virus, human immunodeficiency virus (HIV), and coronavirus have all been successfully studied in 3D cultures [17]. Recently, Zou et al. [35] developed human adult stem cell (ASC)-derived airway 3D that can be utilized to assess infectivity of emerging influenza viruses to human. Another work by Imle and colleagues introduced a 3D culture of primary human CD4 T lymphocytes as an *ex vivo*

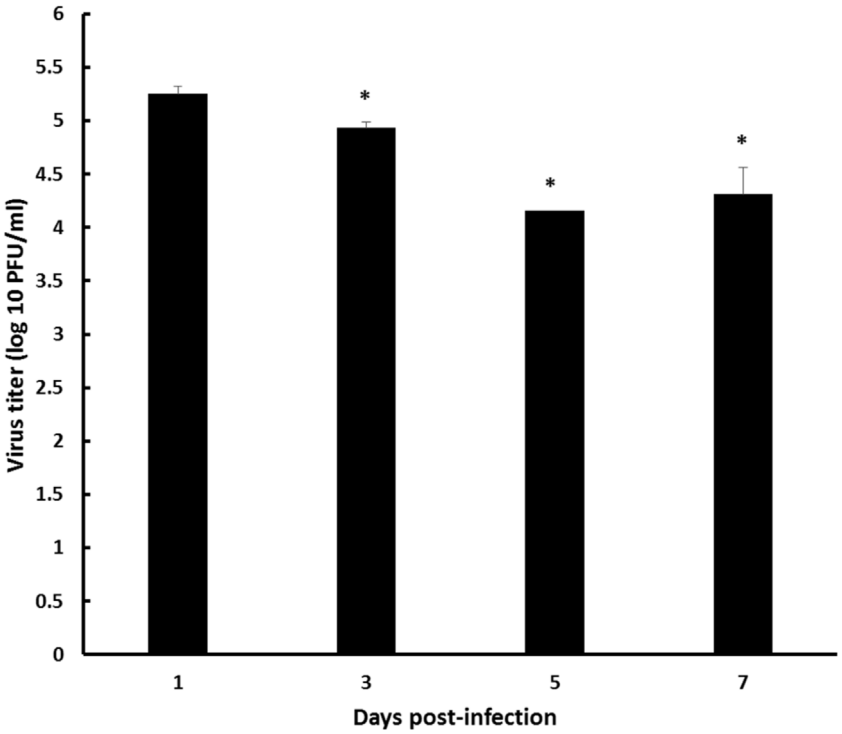

Fig. 4. Growth kinetics of RSVA in A549 spheroids. Spheroids were inoculated with 1 MOI of RSVA and incubated for 7 days. At each of the assigned time-points, 5 infected spheroids were pooled, broken down into cell suspensions, and flash frozen. Virus yield was determined by using plaque assay of the supernatants and cell lysate suspensions at days 1, 3, 5, and 7 post-inoculation. Error bars represent ± SD (n = 3). $^{*}p < 0.05$.

model system to study HIV-1 in tissue-like microenvironments [36]. Here, we established a simple and economic 3D spheroid culture of alveolar type II epithelial cells (A549) as a model to study RSV infection. This culture model can provide a tool for investigating the cellular and molecular mechanisms underlying RSV pathogenesis and to potentially test the effectiveness of antiviral molecules.

Syncytia formation and excessive mucin (MUC1) production are the hallmarks of RSV infection *in vivo* [8,9]. *In vitro*, when A549 monolayers were infected with RSV, MUC1 secretion was only recorded for up to 3 days, after which it started to decline [37,38]. Contrary, studies performed on monolayers of primary human airway epithelial cells report syncytium formation and increased mucin production for up to 6 days post-infection [39–41]. Our results showed that A549 cells grown in spheroids are susceptible and permissive of RSV, which disseminated to the center of the spheroids and induced excessive mucin secretion for up to 7 days post-infection accompanied with syncytia formation. This shows that A549 cells in spheroids behave more closely to primary cells than to A549 monolayers in terms of mucin production and syncytia formation upon RSV infection. Furthermore, we showed that the infection was productive up to day 7 post-inoculation with the virus progressively spreading towards the center of the spheroid. Notably, the virus yield dropped on day by one $\log_{10}$ pfu/ml, which could be explained by the cell death happening at the core of the spheroids. Overall, our data clearly show that A549 spheroids constitute a promising model of RSV infection studies.

To our knowledge, this is the first study to develop a 3D culture model for RSV using alveolar epithelial type II cells and show that infected spheroids display some of the key features of RSV infection *in vivo*, *i.e.*, mucin secretion. Therefore, 3D cultures might be a promising *in vitro* model candidate for studying RSV that can bridge the gap between monolayers and *in vivo* models due to its permissiveness, sustainability of RSV infection, and its ability to recapitulate the lung epithelial tissue's response to infection. More importantly, they are cheap and simple to generate. However, this model is not without its limitations such as the lack of vasculature, tissue heterogeneity and fluid flows observed *in vivo*. Therefore, more work is required to make these 3D cultures ideal model systems to study virus-host interactions and maximize their translational utility.

Funding

The study was supported by the Council for Scientific Research in Lebanon (CNRS-L) and the Medical Practice Plan (MPP) fund, American University of Beirut, Lebanon.

Competing interests

None declared.

Ethical approval

Not required.

Acknowledgment

We thank the DTS core facilities at the Faculty of Medicine, American University of Beirut.

References

[1] World Health Organization. Respiratory Syncytial Virus (RSV). http://www.who.int/influenza/rsv/en/ [Accessed 27 February 2020].
[2] Abou-El-Hassan H, Massaad E, Soudani N, Assaf-Casals A, Shaker R, Lteif Khoury M, et al. Detection of ON1 and novel genotypes of human respiratory syncytial virus and emergence of palivizumab resistance in Lebanon. PLoS One 2019;14:e0212687, http://dx.doi.org/10.1371/journal.pone.0212687.
[3] Hall CB, Long CE, Schnabel KC. Respiratory syncytial virus infections in previously healthy working adults. Clin Infect Dis 2001;33:792–6, http://dx.doi.org/10.1086/322657.

[4] Broor S, Parveen S, Maheshwari M. Respiratory syncytial virus infections in India: epidemiology and need for vaccine. Indian J Med Microbiol 2018;36:458–64, http://dx.doi.org/10.4103/ijmm.IJMM_19_5.
[5] Collins PL, Graham BS. Viral and host factors in human respiratory syncytial virus pathogenesis. J Virol 2008;82:2040–55, http://dx.doi.org/10.1128/JVI.01625-07.
[6] Johani SA, Akhter J. Virology and molecular epidemiology of respiratory syncytial virus (RSV). In: Respiratory disease and infection—a new insight; 2013, http://dx.doi.org/10.5772/53916.
[7] Tregoning JS, Schwarze J. Respiratory viral infections in infants: causes, clinical symptoms, virology, and immunology. Clin Microbiol Rev 2010;23:74–98, http://dx.doi.org/10.1128/CMR.00032-09.
[8] Johnson JE, Gonzales RA, Olson SJ, Wright PF, Graham BS. The histopathology of fatal untreated human respiratory syncytial virus infection. Mod Pathol 2007;20:108–19, http://dx.doi.org/10.1038/modpathol.3800725.
[9] Meng J, Stobart CC, Hotard AL, Moore ML. An overview of respiratory syncytial virus. PLoS Pathog 2014;10:e1004016, http://dx.doi.org/10.1371/journal.ppat.1004016.
[10] Saleh FA, Genever PG. Turning round: multipotent stromal cells, a three-dimensional revolution? Cytotherapy 2011;13:903–12, http://dx.doi.org/10.3109/14653249.2011.586998.
[11] Cukierman E, Pankov R, Stevens DR, Yamada KM. Taking cell-matrix adhesions to the third dimension. Science 2001;294:1708–12, http://dx.doi.org/10.1126/science.1064829.
[12] Voytik-Harbin SL. Chapter 26 three-dimensional extracellular matrix substrates for cell culture. Methods in cell biology, 63. Academic Press; 2001. p. 561–81, http://dx.doi.org/10.1016/S0091-679X(01)63030-9.
[13] Baharvand H, Hashemi SM, Ashtiani SK, Farrokhi A. Differentiation of human embryonic stem cells into hepatocytes in 2D and 3D culture systems in vitro. Int J Dev Biol 2004;50:645–52, http://dx.doi.org/10.1387/ijdb.052072hb.
[14] Loessner D, Stok KS, Lutolf MP, Hutmacher DW, Clements JA, Rizzi SC. Bioengineered 3D platform to explore cell-ECM interactions and drug resistance of epithelial ovarian cancer cells. Biomaterials 2010;31:8494–506, http://dx.doi.org/10.1016/j.biomaterials.2010.07.064.
[15] Barrila J, Radtke AL, Crabbé A, Sarker SF, Herbst-Kralovetz MM, Ott CM, et al. Organotypic 3D cell culture models: using the rotating wall vessel to study host–pathogen interactions. Nat Rev Microbiol 2010;8:791–801, http://dx.doi.org/10.1038/nrmicro2423.
[16] Warren CA, Destura RV, Sevilleja JEAD, Barroso LF, Carvalho H, Barrett LJ, et al. Detection of epithelial cell injury and quantification of infection in the HCT8 organoid model of cryptosporidiosis. J Infect Dis 2008;198:143–9, http://dx.doi.org/10.1086/588819.
[17] He B, Chen G, Zeng Y. Three-dimensional cell culture models for investigating human viruses. Virol Sin 2016;31:363–79, http://dx.doi.org/10.1007/s12250-016-3889-z.
[18] Straub TM, Höner zu Bentrup K, Coghlan PO, Dohnalkova A, Mayer BK, Bartholomew RA, et al. In vitro cell culture infectivity assay for human noroviruses. Emerg Infect Dis 2007;13:396–403, http://dx.doi.org/10.3201/eid1303.060549.
[19] Sainz B, TenCate V, Uprichard SL. Three-dimensional Huh7 cell culture system for the study of Hepatitis C virus infection. Virol J 2009;6:103, http://dx.doi.org/10.1186/1743-422X-6-103.
[20] Saleh FA, Frith JE, Lee JA, Genever PG. Three-dimensional in vitro culture techniques for mesenchymal stem cells. Methods Mol Biol 2012;916, http://dx.doi.org/10.1007/978-1-61779-980-8-4.
[21] Domachowske JB, Bonville CA, Rosenberg HF. Animal models for studying respiratory syncytial virus infection and its long term effects on lung function. Pediatr Infect Dis J 2004;23:S228, http://dx.doi.org/10.1097/01.inf.0000144672.81955.a4.
[22] van Drunen Littel-van den Hurk S, Watkiss ER. Pathogenesis of respiratory syncytial virus. Curr Opin Virol 2012;2:300–5, http://dx.doi.org/10.1016/j.coviro.2012.01.008.
[23] Stittelaar KJ, de Waal L, van Amerongen G, Veldhuis Kroeze EJB, Fraaij PLA, van Baalen CA, et al. Ferrets as a novel animal model for studying human respiratory syncytial virus infections in immunocompetent and immunocompromised hosts. Viruses 2016;8, http://dx.doi.org/10.3390/v8060168.
[24] Taylor G. Animal models of respiratory syncytial virus infection. Vaccine 2017;35:469–80, http://dx.doi.org/10.1016/j.vaccine.2016.11.054.
[25] Heylen E, Neyts J, Jochmans D. Drug candidates and model systems in respiratory syncytial virus antiviral drug discovery. Biochem Pharmacol 2017;127:1–12, http://dx.doi.org/10.1016/j.bcp.2016.09.014.
[26] Chan KF, Carolan LA, Druce J, Chappell K, Watterson D, Young P, et al. Pathogenesis, humoral immune responses, and transmission between cohoused animals in a ferret model of human respiratory syncytial virus infection. J Virol 2018;92, http://dx.doi.org/10.1128/JVI.01322-17.
[27] dit Faute MA, Laurent L, Ploton D, Poupon M-F, Jardillier J-C, Bobichon H. Distinctive alterations of invasiveness, drug resistance and cell-cell organization in 3D-cultures of MCF-7, a human breast cancer cell line, and its multidrug resistant variant. Clin Exp Metastasis 2002;19:161–8.
[28] Gaedtke L, Thoenes L, Culmsee C, Mayer B, Wagner E. Proteomic analysis reveals differences in protein expression in spheroid versus monolayer cultures of low-passage colon carcinoma cells. J Proteome Res 2007;6:4111–8, http://dx.doi.org/10.1021/pr0700596.
[29] Edmondson R, Broglie JJ, Adcock AF, Yang L. Three-dimensional cell culture systems and their applications in drug discovery and cell-based biosensors. Assay Drug Dev Technol 2014;12:207–18, http://dx.doi.org/10.1089/adt.2014.573.
[30] Takai A, Fako V, Dang H, Forgues M, Yu Z, Budhu A, et al. Three-dimensional organotypic culture models of human hepatocellular carcinoma. Sci Rep 2016;6:21174, http://dx.doi.org/10.1038/srep21174.
[31] Fang Y, Eglen RM. Three-dimensional cell cultures in drug discovery and development. SLAS Discov 2017;22:456–72, http://dx.doi.org/10.1177/1087057117696795.
[32] Mazzocchi A, Votanopoulos K, Skardal A. Personalizing cancer treatments empirically in the laboratory: patient-specific tumor organoids for optimizing precision medicine. Curr Stem Cell Rep 2018;4:97–104, http://dx.doi.org/10.1007/s40778-018-0122-z.
[33] Nickerson CA, Goodwin TJ, Terlonge J, Ott CM, Buchanan KL, Uicker WC, et al. *Salmonella enterica*Three-dimensional tissue assemblies: novel models for the study of serovar typhimurium pathogenesis. Infect Immun 2001;69:7106–20, http://dx.doi.org/10.1128/IAI.69.11.7106-7120.2001.
[34] Carterson AJ, Höner zu Bentrup K, Ott CM, Clarke MS, Pierson DL, Vanderburg CR, et al. A549 lung epithelial cells grown as three-dimensional aggregates: alternative tissue culture model for pseudomonas aeruginosa pathogenesis. Infect Immun 2005;73:1129–40, http://dx.doi.org/10.1128/IAI.73.2.1129-1140.2005.
[35] Zhou J, Li C, Sachs N, Chiu MC, Wong BH-Y, Chu H, et al. Differentiated human airway organoids to assess infectivity of emerging influenza virus. PNAS 2018;115:6822–7, http://dx.doi.org/10.1073/pnas.1806308115.
[36] Imle A, Kumberger P, Schnellbächer ND, Fehr J, Carrillo-Bustamante P, Ales J, et al. Experimental and computational analyses reveal that environmental restrictions shape HIV-1 spread in 3D cultures. Nat Commun 2019;10:2144, http://dx.doi.org/10.1038/s41467-019-09879-3.
[37] Li Y, Dinwiddie DL, Harrod KS, Jiang Y, Kim KC. Anti-inflammatory effect of MUC1 during respiratory syncytial virus infection of lung epithelial cells in vitro. Am J Physiol Lung Cell Mol Physiol 2010;298:L558–63, http://dx.doi.org/10.1152/ajplung.00225.2009.
[38] Baños-Lara MDR, Piao B, Guerrero-Plata A. Differential mucin expression by respiratory syncytial virus and human metapneumovirus infection in human epithelial cells. Mediators Inflamm 2015;2015:347292, http://dx.doi.org/10.1155/2015/347292.
[39] Tristram DA, Hicks W, Hard R. Respiratory syncytial virus and human bronchial epithelium. Arch Otolaryngol Head Neck Surg 1998;124:777–83.
[40] Villenave R, Thavagnanam S, Sarlang S, Parker J, Douglas I, Skibinski G, et al. In vitro modeling of respiratory syncytial virus infection of pediatric bronchial epithelium, the primary target of infection in vivo. PNAS 2012;109:5040–5, http://dx.doi.org/10.1073/pnas.1110203109.
[41] Guo-Parke H, Canning P, Douglas I, Villenave R, Heaney LG, Coyle PV, et al. Relative respiratory syncytial virus cytopathogenesis in upper and lower respiratory tract epithelium. Am J Respir Crit Care Med 2013;188:842–51, http://dx.doi.org/10.1164/rccm.201304-0750OC.